Elucidating the relationship between states of water and ion transport properties in hydrated polymers

Thien Tran, Chen Lin, Shabdiki Chaurasia, and Haiqing Lin*

Department of Chemical and Biological Engineering, University at Buffalo, The State University of New York, Buffalo, NY 14260, USA.

*Corresponding author. Tel: +1-716-645-1856, Email: haiqingl@buffalo.edu (H. Lin)

Resubmission to *Journal of Membrane Science*

9/30/2018

Abstract: Ions transport properties in hydrated polymers is usually correlated with the amount of water assuming that all water contributes equally. Herein, we demonstrate that water in polymers exists in three states (non-freezable, intermediate, and free water), and the different states of water exert different impacts on polymer properties including glass transition temperature and ion sorption and diffusion. We synthesized four systematic series of polymer networks including neutral, zwitterionic, cation exchange, and anion exchange polymers. The amounts of water in different states in the hydrated polymers were determined using Differential Scanning Calorimetry (DSC), and their dependence on the polymer composition is investigated. The glass transition temperature of the hydrated polymers is satisfactorily correlated with the non-freezable water using the Gordon-Taylor equation. The salt solubility is correlated with the combined free and intermediate water, and the salt diffusivity is satisfactorily correlated with the total water using the modified Yasuda model.

Graphical abstract

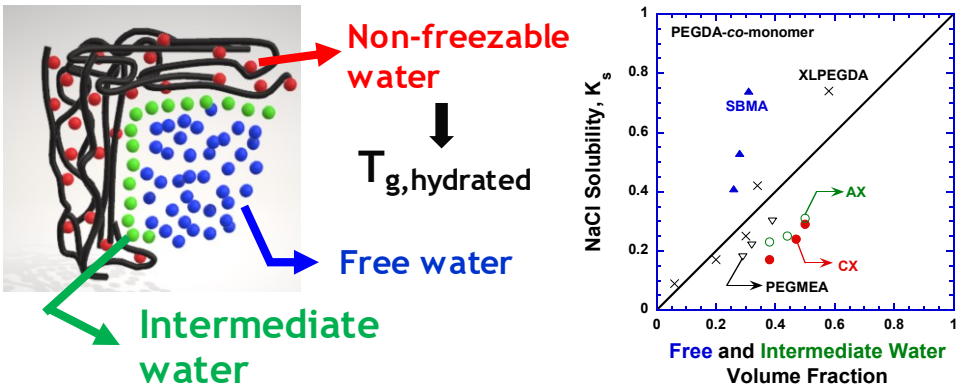

Keywords: State of water; charged polymers; glass transition temperature; salt sorption and diffusion; freezable water

1. INTRODUCTION

The sorption and diffusion of water and ions in hydrated polymers is central to a variety of membrane applications, such as reverse osmosis [1-3], forward osmosis [4, 5], nanofiltration [6], ultrafiltration [7, 8], electrodialysis [9], facilitated gas separation [10], and fuel cells [11-13]. These polymers can be neutral [14, 15], cation exchange [16-18], anion exchange [19, 20], or zwitterionic [21, 22]. The solubility and diffusivity of the ions are determined by the amount of water within the polymers [23, 24] and chemical structures (such as cross-linking density [14, 15] and ionic groups [19, 20]). Understanding the role of the water in small molecule transport is critical to designing high-performance polymers with controlled water and ion transport properties.

Salt solubility (K_S) in hydrated polymers is usually defined as follows [5, 25]:

$$K_S = \frac{C_S^m}{C_S} \tag{1}$$

where C_S^m and C_S are the salt concentration in the swollen polymer and the equilibrium aqueous solution, respectively. Because the salt has negligible solubility in neutral polymer chains, K_S often equals to v_W, the volume fraction of water in the hydrated polymers. However, the presence of the polymer chains often suppresses the salt sorption, resulting in lower K_S values than v_W.

Salt diffusion coefficient (D_S, cm^2/s) in the neutral polymers can be described using the modified Yasuda equation [26, 27]:

$$D_S = D_S^0 exp\left[b\left(1 - \frac{1}{v_W}\right)\right] \tag{2}$$

where D_S^0 is the salt diffusion coefficient in pure water, and b is an adjustable constant related to the size of the salt. The v_W also represents the free volume in the hydrated polymers available for the water and salt diffusion.

For charged networks, the transport of ions is strongly influenced by the fixed charged groups on the polymer chains [19, 20, 22, 28, 29]. Recently, Freeman and coworkers have

developed a theoretical framework using the Donnan theory and Manning model to predict the salt sorption, and the Mackie and Meares model to predict the ion diffusivity in charged polymers [19, 20, 30]. The dissociated counter-ions in polyelectrolytes induce osmotic pressure, increasing the degree of swelling and thus the diffusivity of ions and water [24, 31].

Although the models above could describe the transport properties of ions in hydrated polymers, they treat water in the polymer networks equally. However, water in hydrophilic polymers usually exists in three states: non-freezable water, intermediate (freezing bound) water, and free water [12, 32-34]. Non-freezable water strongly interacts with hydrophilic groups of the polymers via hydrogen bonding or electrostatic forces, and therefore, it does not crystallize at temperatures as low as 200 K [32, 35]. Free water is unbounded and exhibits freezing point and crystallization enthalpy similar to pure water. Intermediate water weakly interacts with the polymers or the non-freezable water and often has a melting temperature below 273 K [35]. The combined free and intermediate water is known as the freezable water.

Considering the different states of water, the hydrated polymers should contain three separated macro-phases, free water, one phase containing the polymer and non-freezable water, and intermediate water. The water in different states is expected to exert different effects on the polymer properties. For example, the glass transition temperature (T_g) of a hydrated polymer should be determined by the non-freezable water, instead of the total water content in the polymers. The intermediate water was suggested to determine the biocompatibility of the polymers and possibly the antifouling properties [36, 37]. However, there lacks systematic studies of the effect of different states of water on the properties of the hydrated polymers including the ion solubility and permeability.

In this work, we synthesized the neutral, charged, and zwitterionic polymer networks using the representative cross-linker and monomers (as shown in Table 1) by the free radical polymerization [38]. Poly(ethylene glycol) diacrylate (PEGDA) is a neutral cross-linker to prepare hydrophilic networks containing mainly ethylene oxide (EO) repeating units [14, 39, 40]. Poly(ethylene glycol) methyl ether acrylate (PEGMEA) with an EO content similar to PEGDA provides a baseline of neutral networks to understand the effect of cross-linking density on the polymer properties. Zwitterionic materials derived from sulfobetaine methacrylate (SBMA) exhibit ultralow fouling behavior because of their strong interactions with water by electrostatic force and the resulting hydration layer mitigating the adhesion of foulants [41, 42]. Polyelectrolytes derived from 2-acrylamido-2-methyl-1-propanesulfonate sodium (AMPS) or [2-(acryloyloxy)ethyl] trimethyl ammonium chloride (AETMAC) are used to investigate the dependence of the ion transport properties on the fixed charged groups on the polymer backbones. These series of cross-linked polymers derived from PEGDA and monomers with various ionic groups provide space to explore the relationship of the structure and properties.

This work, for the first time, systematically elucidates the effect of the states of water on the physical properties and salt transport properties in four series of hydrated polymer networks, neutral PEGDA-*co*-PEGMEA copolymers, anion exchange PEGDA-*co*-AX, cation exchange PEGDA-*co*-CX, and zwitterionic PEGDA-*co*-SBMA. The states of water were determined using Differential Scanning Calorimetry (DSC). In contrast to conventional studies based on the total water content, the T_g of the hydrated polymers is successfully correlated with the content of the non-freezable water using the Gordon-Taylor equation, and the salt solubility is correlated with the content of the freezable water. Interestingly, the salt diffusivity is related to the total water content (instead of the freezable water content) using the free volume model.

Table 1. Chemical Structure of Representative Cross-linker and Monomers.

Cross-linker/monomer	Properties	Chemical Structure
Poly(ethylene glycol) diacrylate (PEGDA)	Neutral cross-linker	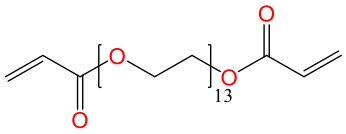
Poly(ethylene glycol) methyl ether acrylate (PEGMEA)	Neutral monomer	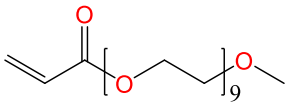
Sulfobetaine methacrylate (SBMA)	Zwitterionic	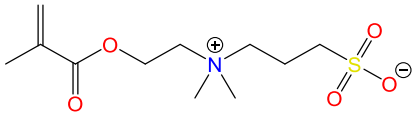
2-Acrylamido-2-methyl-1-propanesulfonate sodium (AMPS)	Negatively charged (cation exchange, CX)	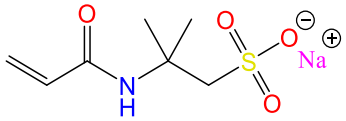
[2-(Acryloyloxy)ethyl] trimethyl ammonium chloride (AETMAC)	Positively charged (anion exchange, AX)	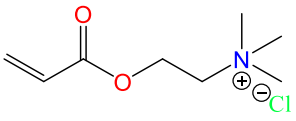

2. EXPERIMENTAL SECTION

2.1. Materials

PEGDA (Mn =700 g/mol), PEGMEA (Mn = 480 g/mol), SBMA, AMPS (50 wt.% in H_2O), AETMAC (80 wt.% in H_2O), and the initiator, 1-hydroxycyclohexyl phenyl ketone (HCPK), were purchased from Sigma-Aldrich Chemical (Milwaukee, WI) and used as received. Deionized water was generated by Milli-Q water equipment (18.2 MΩ/cm at 23.8 °C) (EMD Millipore, Billerica, MA).

2.2. Preparation of polymer networks

Freestanding films of the polymer networks were prepared by UV photopolymerization using prepolymer solutions containing the required amounts of the cross-linker and monomer in 50 wt.% aqueous solutions [14, 22, 38]. To prepare a prepolymer solution, the initiator (HCPK) was dissolved in PEGDA (0.1 wt.% relative to PEGDA) while the monomer was dissolved in Milli-Q water. The PEGDA solution was then added to the monomer solution to form a solution containing 50 wt.% water. After stirring, the solution was sonicated for about 10 min to eliminate air bubbles in an Ultrasonic cleaner (Model FS60, Fisher Scientific, Pittsburgh, PA). To prepare a freestanding film, the solution was sandwiched between two quartz plates, which were separated by spacers to control the film thickness. The assembly was exposed to 365-nm UV light in a chamber (Model CX-2000 UV Crosslinker, UVP) for 5 min for polymerization. The obtained solid film was then removed from the plates and kept in DI water for at least 24 h to remove the unreacted monomer or sol. The obtained copolymer network is labeled as PEGDA-*co*-monomerxx, where "xx" indicates the weight percentage of the monomer (PEGMEA, SBMA, AMPS, or AETMAC) in the copolymers on the dry basis.

2.3. Water sorption and physical properties characterization

The conversion of (meth)acrylate groups in the PEGDA and monomers was determined using attenuated total reflection Fourier transform infrared (ATR-FTIR) spectroscopy (Bruker Vertex 70, Billerica, MA) [14, 22].

The gel content of the polymers was determined using a solvent extraction method [14, 22]. After the polymerization, the film was dried and weighed (with a mass of m_0). After immersion in the DI water overnight to remove the sol, the film was dried and weighed again (with a mass of m_{gel}). The gel weight percentage (w_{gel}) is calculated using Eq. (3) [5, 22]:

$$w_{gel} = \frac{m_{gel}}{m_0} \times 100\% \quad (3)$$

The equilibrium water uptake (W_W, g H_2O/g dry polymer) of the polymer is calculated using the following equation [22, 38, 43]:

$$W_W = \frac{m_{wet} - m_{dry}}{m_{dry}} \quad (4)$$

where m_{wet} and m_{dry} are the weight of the hydrated and dry polymer, respectively. The m_{dry} was determined after the film was dried in a vacuum oven at 60 °C for 24 h. The polymer samples had a dry weight of 150 – 400 mg. For each copolymer, three samples were test, and the mean values are reported as well as the standard deviation.

The density of the dry polymers was determined using an analytical balance equipped with a density kit (XS 64, Mettler Toledo Inc., Columbus, OH). Iso-octane was used as an auxiliary liquid. The polymer density (ρ_P, g/cm^3) was calculated by the following equation [14]:

$$\rho_P = \frac{m_{dry}}{m_{dry} - m_{liq}} \rho_{liq} \quad (5)$$

where m_{liq} is the weight of the polymer in iso-octane, and ρ_{liq} is the density of iso-octane.

The absorbed water in the polymers is assumed to have the same density as the free water (ρ_W = 1.0 g/cm^3). Therefore, the water volume fraction (v_W) in the hydrated polymers can be calculated using Eq. (6):

$$v_W = \frac{(m_{wet} - m_{dry})/\rho_W}{(m_{wet} - m_{dry})/\rho_W + m_{dry}/\rho_P} = \frac{W_W/\rho_W}{W_W/\rho_W + 1/\rho_P} \quad (6)$$

2.4. Determination of the states of water

The states of water in the polymer networks were quantitatively determined using DSC (Q2000, TA Instruments, New Castle, DE). The fully hydrated sample was placed in an aluminum pan and hermetically sealed. For scanning, the sample was cooled to -80 °C at 20 °C/min and then kept at -80 °C for 5 min before heating to 40 °C at 2.0 °C/min under a nitrogen atmosphere.

The content of the freezable water (W_f, g H_2O/g dry polymer) was calculated from the water melting enthalpy (ΔH_m, J/g) assuming that both free water and intermediate water have the same melting enthalpy as pure water ($\Delta H_{H_2O}^m$= 333.5 J/g) [44-46]:

$$W_f = W_{im} + W_{free} = \frac{\Delta H_m}{\Delta H_{H_2O}^m}(1 + W_W) \quad (7)$$

where W_{free} and W_{im} are the content of the free and intermediate water in the dry polymer (g H_2O/g dry polymer), respectively.

The W_{im} values can be calculated using the crystallization enthalpy (ΔH_c, J/g) for the combined cooling and heating crystallization peaks:

$$W_{im} = \frac{\Delta H_c}{\Delta H_{H_2O}^m}(1 + W_W) \quad (8)$$

The amount of the non-freezable water (W_{nf}) can be calculated using Eq. (9):

$$W_{nf} = W_W - W_f \quad (9)$$

The T_g of the dry and hydrated polymers can also be determined using the DSC. The T_g value is chosen as the midpoint of the step change of the heat capacity using the Universal Analysis software (TA Instruments). The cold crystallization temperature (T_{cc}) of the water in the hydrated polymers is determined by the exothermic peak during the heating scanning.

2.5. Characterization of salt transport properties

The salt diffusion coefficient and solubility were determined using kinetic desorption experiments [5, 17]. The hydrated polymer films were cut into disks (with 0.75-inch in diameter and a thickness of 350 – 500 μm depending on the degree of swelling) and then equilibrated with 100 ml of 0.5 M NaCl solution. The sample was then taken out of the NaCl solution, and the liquid on the surface was removed before it was immersed in 35 ml of DI water. A conductivity probe (CON-BTA, Vernier Software & Technology, Beaverton, OR) was used to monitor the NaCl

content in the extracting solution as a function of time. The NaCl diffusion coefficient was calculated using the Fickian diffusion model [5, 15, 27]:

$$D_S = 0.196l^2 \left[\frac{d(M_t/M_\infty)}{d(t^{1/2})}\right]^2 \quad (10)$$

where l is the thickness of the swollen film (cm), and M_t (g) and M_∞ (g) are the mass of NaCl in the extracting solution at time t (s) and equilibrium, respectively. The extraction is assumed to completely remove the NaCl from the polymer, and thus the M_∞ value equals the initial NaCl mass in the hydrated polymer before the desorption.

The K_S value was calculated using the following equation:

$$K_S = \frac{C_S^m}{C_S} = \frac{M_\infty}{V_P C_S} \quad (11)$$

where V_P is the volume of the swollen polymer sample, and C_S is 0.5 M or 29.2 g/L in this study.

3. RESULTS AND DISCUSSION

3.1. Physical characterization of polymer networks

The conversion of (meth)acrylate groups in PEGDA and monomers was confirmed by ATR-FTIR, as shown in Figure 1. The pre-polymer solution exhibits four characteristic peaks of acrylate groups at 810, 1200, 1410 and 1640 cm^{-1} [5, 14, 22, 38], which disappear after the polymerization, indicating almost complete conversion of (meth)acrylate groups.

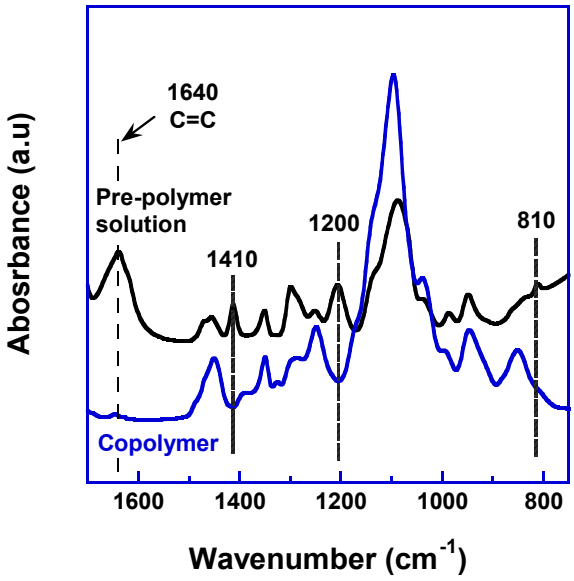

Figure 1. Comparison of FTIR spectra of a pre-polymer solution (containing 50 wt.% H_2O, 40 wt.% PEGDA, and 10 wt.% SBMA), and the resulting copolymer (PEGDA-*co*-SBMA20).

Table 2 summarizes physical properties of the dry polymer networks including gel fraction, density, $T_{g,P}$, W_W, and v_W. The gel content slightly decreases as the monomer content in the copolymer increases. Nevertheless, the gel fraction of all copolymers is 95% or above except for PEGDA-*co*-SBMA50. Assuming that the sol is completely SBMA for the PEGDA-co-SBMA50, the gel should be still derived from 54 wt.% PEGDA and 46 wt% SBMA, which is less than 10% deviation from the prepolymer composition. Therefore, the gel of these copolymers is assumed to exhibit the same composition as the prepolymer solutions for the convenience of the data analysis. These results are consistent with other studies on the hydrogels, confirming the high conversion of (meth)acrylate group [5, 14, 22, 39]. The v_W increases with decreasing the PEGDA content in the copolymers. For all the polymer networks, v_W is higher than the volume percentage of water in the pre-polymer solutions (*i.e.*, ~50 vol.%), suggesting the absence of polymerization-induced phase separation [14, 39, 47]. Additionally, the dry and hydrated copolymers are transparent,

except for the dry PEGDA-co-SBMA50, which is slightly opaque due to the macroscopic phase-separation.

Table 2. Water Uptake and Physical Properties of the Polymers.

Polymers	w_{gel} (wt.%)	W_W (g g^{-1})	v_W	ρ_P (g/cm^3)	$T_{g,p}$ (K)	T_{cc} (K)	$T_{g,S}$ (K)
XLPEGDA50*	98	1.15 ± 0.03	0.58 ± 0.02	1.18 ± 0.03	233 ± 2	241 ± 1	209 ± 3
PEGDA-*co*-PEGMEA20	99	1.25 ± 0.01	0.60 ± 0.01	1.17 ± 0.04	226 ± 2	240 ± 2	195 ± 4
PEGDA-*co*-PEGMEA35	99	1.41 ± 0.03	0.62 ± 0.01	1.16 ± 0.01	221 ± 1	238 ± 1	205 ± 2
PEGDA-*co*-PEGMEA50	98	1.53 ± 0.02	0.64 ± 0.04	1.16 ± 0.02	218 ± 1	NA†	206 ± 2
PEGDA-*co*-SBMA20	97	1.32 ± 0.05	0.62 ± 0.02	1.21 ± 0.02	240 ± 1	232 ± 3	213 ± 3
PEGDA-*co*-SBMA35	96	1.42 ± 0.07	0.64 ± 0.01	1.24 ± 0.01	240 ± 1	230 ± 2	208 ± 1
PEGDA-*co*-SBMA50	92	1.61 ± 0.04	0.67 ± 0.04	1.26 ± 0.02	239 ± 2	NA†	206 ± 1
PEGDA-*co*-CX20	99	1.67 ± 0.03	0.68 ± 0.01	1.25 ± 0.01	257 ± 2	235 ± 2	211 ± 3
PEGDA-*co*-CX35	96	2.04 ± 0.09	0.73 ± 0.01	1.29 ± 0.01	282 ± 1	233 ± 3	212 ± 2
PEGDA-*co*-CX50	95	2.61 ± 0.09	0.78 ± 0.01	1.33 ± 0.02	319 ± 5	NA†	238 ± 4
PEGDA-*co*-AX20	99	1.58 ± 0.01	0.66 ± 0.02	1.20 ± 0.02	237 ± 1	225 ± 2	207 ± 2
PEGDA-*co*-AX35	97	1.86 ± 0.05	0.69 ± 0.02	1.21 ± 0.01	282 ± 3	222 ± 1	226 ± 1
PEGDA-*co*-AX50	97	2.25 ± 0.07	0.73 ± 0.05	1.23 ± 0.03	296 ± 4	NA†	226 ± 5

*Prepared from a pre-polymer solution containing 50 wt.% PEGDA and 50 wt.% H_2O.

†NA: not detectable in the DSC scanning.

Table 2 also shows that the density and T_g of PEGDA-*co*-PEGMEA decrease with increasing the PEGMEA content because increasing the content of the flexible $–OCH_3$ chain end groups increases the polymer free volume [48, 49]. For the zwitterionic PEGDA-*co*-SBMA, the density increases with increasing the SBMA content. The T_g of the polySBMA was reported to be 476 K in the literature [50], which is much higher than that determined for PEGDA-*co*-SBMA (~240 K). However, the T_g for polySBMA cannot be determined using DSC in this study because of the degradation temperature at K, as shown in the thermal gravimetric analysis (TGA) in Figure S1b in the Supplemental Information. Nevertheless, the dry PEGDA-co-SBMA are expected to be phase-separated, with the T_g of the PEO phase remaining independent of the SBMA content (~240 K), which is consistent with the literature [22].

Both density and T_g of the charged polymers (PEGDA-*co*-CX and PEGDA-*co*-AX) increase as the content of the charged monomer increases because the electrostatic interactions among ionic groups on the polymer branches increase the stiffness of the polymer chains and tighten the structures.

3.2. Water sorption and states of water in the polymer networks

Figure 2 presents the effect of the PEGDA content in the polymers on the equilibrium water uptake (W_W). Because all prepolymer solutions contained 50 wt% water, the PEGDA content in the polymer (twice the value of that in the prepolymer) serves as a good indicator for the cross-linking density [14]. For example, PEGDA-*co*-PEGMEA copolymers have very similar EO content (82%), while decreasing the PEGDA content increases the water uptake because of the decrease in the cross-linking density [14, 47]. All other copolymers exhibit the similar trend, i.e., decreasing PEGDA content increases water sorption because of the decrease in cross-linking density and increase in hydrophilicity. At the same PEGDA content, the PEGDA-*co*-CX series

exhibit the highest W_W values, followed by PEGDA-*co*-AX because of the higher content of ionic groups, or the osmotic pressure induced by the counterions [31]. The zwitterionic PEGDA-*co*-SBMA exhibit the W_W values unexpectedly similar to the PEGDA-*co*-PEGMEA, despite the positive and negative charges on the side chains.

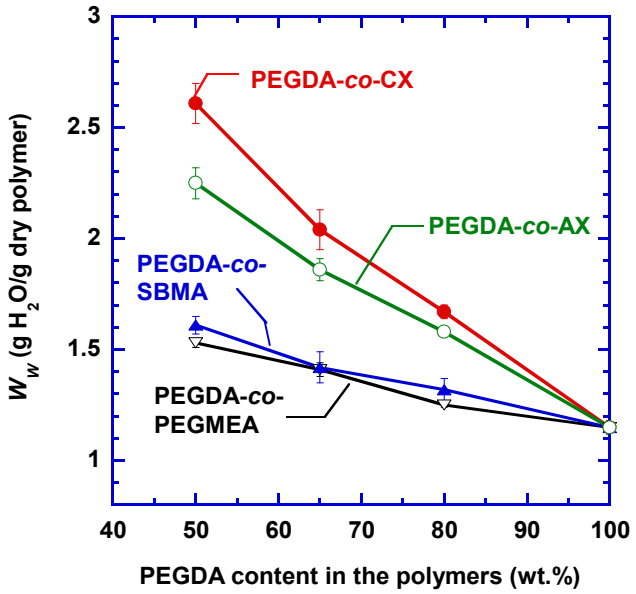

Figure 2. Effect of the PEGDA content in the copolymers on the equilibrium water uptake (W_W) at 21 °C. The pre-polymer solution contains 50 wt.% water.

Figure 3a shows the DSC thermograms of four representative dry copolymers of PEGDA-*co*-monomer20. There is no endothermic or exothermic peak observed, suggesting that these polymers are amorphous in the temperature range studied (200 – 320 K). Figure 3b discloses a full cycle (cooling and heating) of a DSC scan for one sample (PEGDA-*co*-PEGMEA20). As the sample is cooled to -80 °C at 20 °C/min, the free water crystallizes at ~255 K, and then a part of the intermediate water crystallizes at ~220 K. The other part of intermediate water crystallizes at ~233 K during the heating cycle [36, 37, 44]. The combined enthalpy changes (ΔH_c) can be used to calculate the amount of intermediate water by Eq. (8). As the temperature further increases, the

free and intermediate water melt at ~273 K [33, 35, 51], and the enthalpy of melting can be used to determine the freezable water content using Eq. (7).

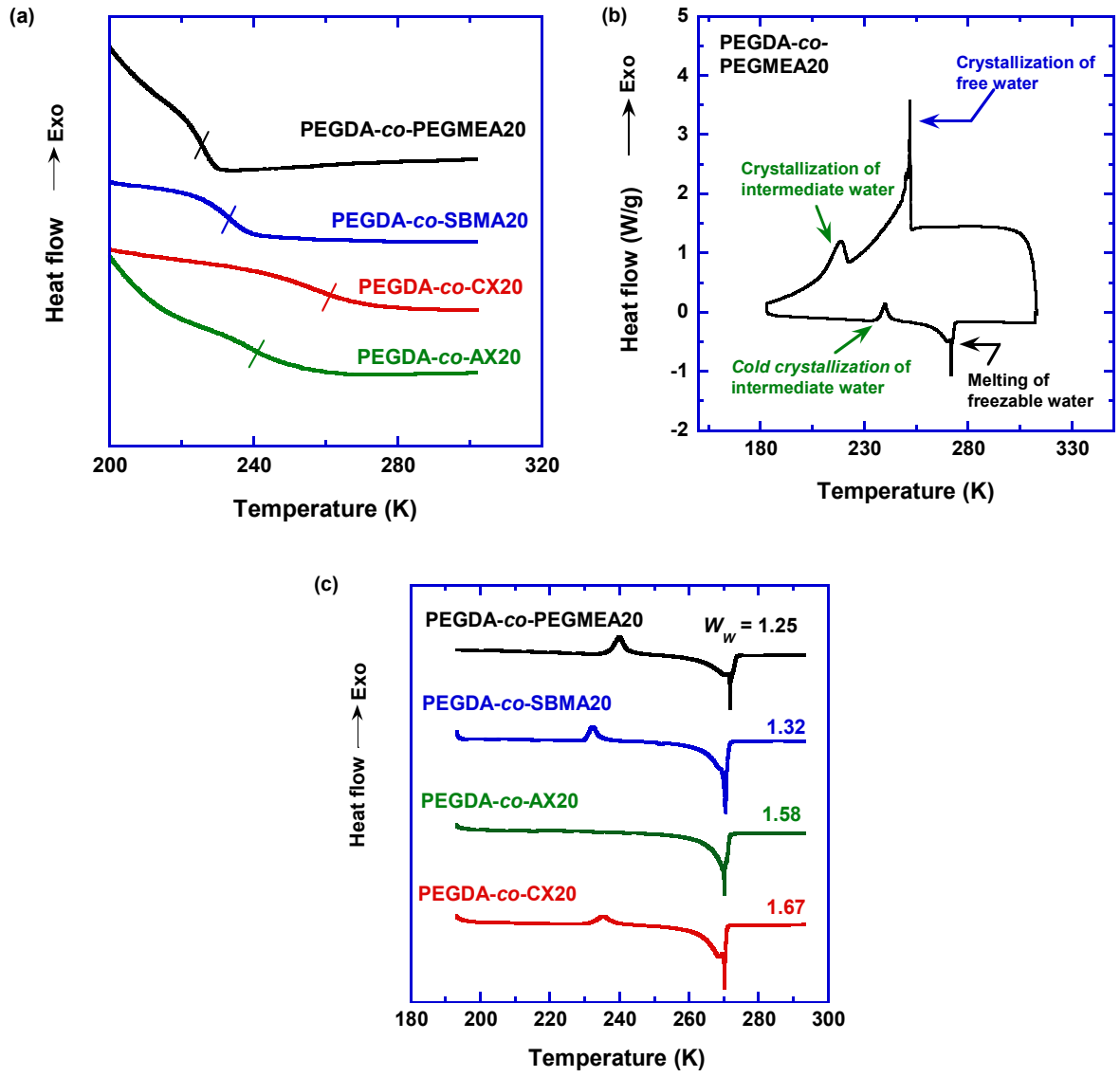

Figure 3. DSC thermograms of (a) the dry copolymers of PEGDA-*co*-monomer20, (b) an example hydrated PEGDA-*co*-PEGMEA20 for a full cooling and heating cycle, and (c) the hydrated copolymers of PEGDA-*co*-monomer20 during the heating step. The thermograms of other copolymers can be found in Figure S1 of the Supplemental Information.

Figure 3c shows the thermograms of four hydrated PEGDA-*co*-monomer20 copolymers during the heating cycle. Similar to Figure 3b, all hydrated polymers exhibit a crystallization peak at 222-240 K (for the intermediate water) and then a melting peak at ~273 K (for the freezable water). The hydrated PEGDA-*co*-PEGMEA20 exhibits slightly higher crystallization and melting temperature of water than the charged and zwitterionic polymers because the ionic groups have a stronger interaction with the intermediate water than the neutral PEGDA-*co*-PEGMEA, facilitating its crystallization and melting (cf. Table 2).

To understand the effect of cross-linking and chemical structure on the states of water in the polymers, the total water sorption is decoupled into the freezable water (W_f) and non-freezable water (W_{nf}). As shown in Figure 4a, the W_f value decreases with increasing the PEGDA content in the polymers, and it decreases in the following order, PEGDA-*co*-CX, PEGDA-*co*-AX > PEGDA-*co*-PEGMEA > PEGDA-*co*-SBMA. Interestingly, the PEGDA-*co*-SBMA copolymers exhibit lower W_f values than PEGDA-*co*-PEGMEA, though the W_W values are similar for both series of copolymers.

The freezable water in the polymers can be further decoupled into the free and intermediate water. As shown in Figure 4b, the W_{free} values decrease with increasing PEGDA content in the polymer, which is similar to that for the W_W values. Increasing the cross-linking density creates more constraint for the polymer gel to swell and thus decreases the W_f values, as exemplified in PEGDA-*co*-PEGMEA. Additionally, the charged polymers (PEGDA-*co*-AX and PEGDA-*co*-CX) exhibit much higher free water content than the zwitterionic and neutral polymers. Interestingly, zwitterionic polymers show the W_{free} values similar to the neutral polymers.

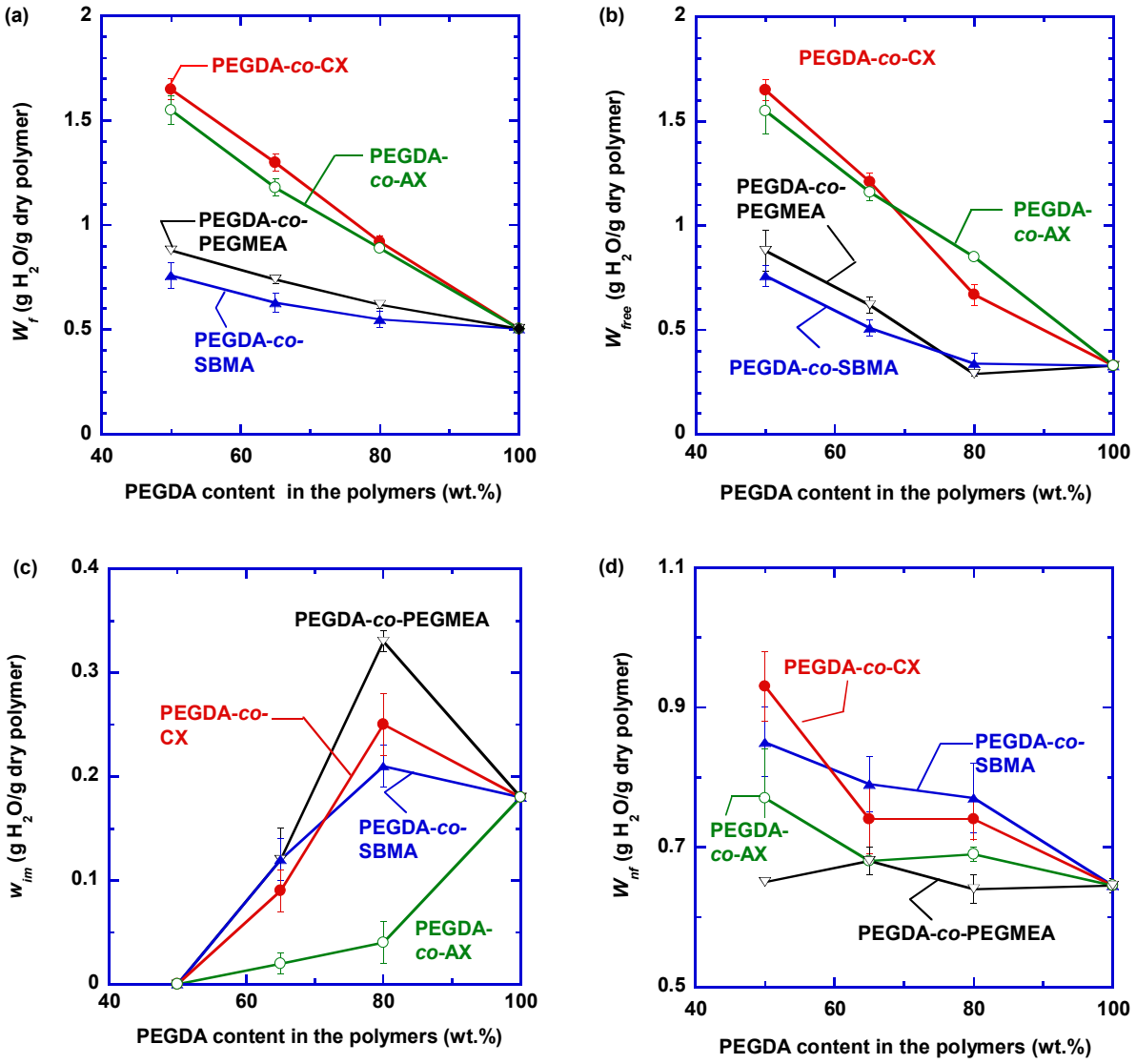

Figure 4. Effect of the PEGDA content in the polymers on (a) the freezable water content (W_f), (b) the free water content (W_{free}), (c) the intermediate water content (W_{im}), and (d) the non-freezable water content (W_{nf}). All the pre-polymer solutions contain 50 wt.% H_2O. The value reported is the average for three samples, and the error bar is the standard deviation.

Figure 4c shows that increasing the PEGDA content in the copolymer unexpectedly increases the W_{im} values before decreasing. All polymers with 50% monomers show the W_{im} values near zero. The W_{im} diminishes as the free water becomes dominant (*i.e.*, $W_f/W_w \geq 50\%$). This

behavior has also been observed in PEG-water and poly(2-methacryloyloxyethyl phosphorylcholine)-water (polyMPC-water) systems [44, 52]. As the water content in PEG-water system increases from 1.8 g g^{-1} to approximately 9.7 g g^{-1}, the W_{im} value decreases from 0.15 to 0.04 [44]. Similarly, when the water content in the polyMPC-water system increases from 0.5 g g^{-1} to 2 g g^{-1}, the W_{im} value decreases from 0.12 to 0 [52]. PEGDA-*co*-PEGMEA20 exhibits the highest W_{im} value (accounting for 53% of the freezable water), while the percentage of W_{im} to W_f for PEGDA-*co*-SBMA20, PEGDA-*co*-CX20, and PEGDA-*co*-AX20 is only 38%, 27%, and 4%, respectively (cf. Table S1 of the Supplemental Information).

Both PEGDA-*co*-CX and PEGDA-*co*-SBMA show similar W_{im} values, which are much higher than those for PEGDA-*co*-AX, presumably because SBMA and AMPS (CX) have SO_3^- end groups with stronger hydration than the $-N^+(CH_3)_3$ groups in the AX. Similar results have been reported in the literature. For example, polyMPC with $-N^+(CH_3)_3$ end groups shows the amount of intermediate water less than 4% of the freezable water at W_W above 1.5 g g^{-1}, and almost 0 at W_W above 2 g g^{-1} [52]. Additionally, the cold crystallization temperature (T_{cc}) of the water in the hydrated polymers appears to increases with increasing the amount of the intermediate water (cf. Table 2).

Figure 4d shows the effect of the PEGDA content in the polymer on the non-freezable water content (W_{nf}). The PEGDA-*co*-PEGMEA copolymers with almost constant EO content exhibit similar W_{nf} values, indicating that the cross-linking density has minimal effect on the W_{nf} values. As the PEGDA content decreases from 100 wt.% to 50 wt.%, the W_{nf} increases by 41% for PEGDA-*co*-CX (from 0.66 g g^{-1} to 0.93 g g^{-1}), by 17% for PEGDA-*co*-AX, and 29% for PEGDA-*co*-SBMA. The ionic groups can form stronger electrostatic interactions with water than EO in PEGMEA, resulting in higher W_{nf} values in the charged and zwitterionic polymers [42, 53, 54].

Because the W_{nf} value is mainly determined by the amount of hydrophilic groups, an additive model can be used to estimate the molar ratio of water to functional groups assuming that the non-freezable water only interacts with the functional groups such as EO and ions, as expressed in Eq. (12).

$$w_{nf} = MW_{water}\left[\frac{13 \cdot w_{PEGDA} \cdot x}{MW_{PEGDA}} + \frac{w_{monomer} \cdot y}{MW_{monomer}}\right] \quad (12)$$

where MW_{water}, MW_{PEGDA}, and $MW_{monomer}$ is the molecular weight of water (18 g/mol), PEGDA (700 g/mol), and the monomer (SBMA, AX or CX), respectively. The number of 13 is the number of EO repeating unit in PEGDA. The x and y are the numbers of mole of non-freezable water per EO repeating unit and monomer, respectively.

Figure 6 compares the modeled and measured W_{nf} values for each copolymer, which are in good agreement. The modeled numbers of moles of water per mole of functional groups (x and y) are recorded in Table 3.

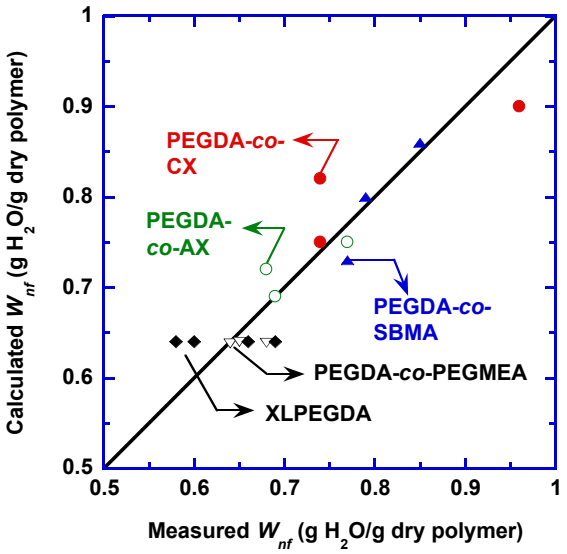

Figure 6. Parity plot between the measured and modelled amount of the non-freezable water (W_{nf}) in the hydrated polymers. XLPEGDA samples were prepared from the pre-polymer solutions containing various amount of water (50, 60, 67.5, and 75 wt.%).

Table 3. Estimated Moles of Non-freezable Water Per Mole of the Monomer/Ion.

Monomer/ions	EO	SBMA	AMPS (CX)	AETMAC (AX)	$-SO_3^-$	$-N^+(CH_3)_2-$
This study	1.9±0.2	17±1	15±1	9.1±0.5	9-10	7-8
Literature values	2.0 [55], 2.7 [56], 1.0 [57, 58]	25.7 [59], ~8 [57]			7.1 [59] 8-14 [60]	18.6 [59]

Each EO repeating unit interacts with 1.9 ± 0.2 water molecules, which is consistent with the literature value of 2.0 obtained using DSC [55, 56], though a value of 1.0 was also reported in the study of Nuclear Magnetic Resonance (NMR) [57, 58]. Each SBMA unit interacts with 17 ± 1 water molecules confirming the stronger electrostatic interactions between water and $-SO_3^-$ or $-N^+(CH_3)_2-$ ions than the interaction between water and EO. The value of 17 is very close to the literature value of 25.7 derived from a simulation of the coordination number of water molecules in the first coordination shell of SBMA [59]. However, a value of ~8 was also reported in an NMR study [57].

The cationic AMPS in the PEGDA-*co*-CX series binds 15 ± 1 water molecules, which is comparable to that of SBMA, partially due to the same anionic $-SO_3^-$ groups. The Na^+ ions have been widely reported to have a hydration number of 5-6 [61, 62]. Therefore, each $-SO_3^-$ group can attract 9-10 water molecules, which is close to a value of 7 in the simulation study [59, 63]. On the other hand, each $-N^+(CH_3)_2-$ group is estimated to bind 7-8 water molecules, which is lower than that reported in the simulation study (18.6) [59].

Each AETMAC monomer in PEGDA-*co*-AX binds 9.2 ± 0.5 water molecules. The amount of strongly bound water in AETMAC is mostly ascribed to the free counter ion (Cl^-) with a

hydration number of 6-7 [61, 64]. Consequently, each -$N^+(CH_3)_3$ cation is estimated to bind only 2-3 water molecules, which is much lower than the –$N^+(CH_3)_2$– group in SBMA.

In summary, the estimation of the non-freezable water using DSC in this study is in good agreement with the literature studies with DSC studies, and disagreement with other literature using different techniques (such as NMR and simulation). Such discrepancy has been reported for PEO, which was ascribed to the methods NMR adopts to detect water [57]. Nevertheless, our study convincingly confirms that the charged and zwitterionic polymers exhibit more non-freezable water than EO.

3.3. Correlation of water sorption and T_g of the polymer networks

Conventionally, the glass transition temperature of hydrated polymers ($T_{g,S}$) is related to the total water content using the Gordon-Taylor equation [65, 66]. However, based on the different states of water in the polymer, the $T_{g,S}$ should be related to the amount of non-freezable water in the polymer:[67]

$$T_{g,S} = \frac{w'_{nf} T_{g,H_2O} + K w'_P T_{g,P}}{w'_{nf} + K w'_P} \quad (13)$$

where K is an adjustable parameter, and $T_{g,P}$ and T_{g,H_2O} are the T_g for the dry polymer and pure water (*i.e.*, 135 K [45]), respectively. The $T_{g,P}$ values have been recorded in Table 1. The w'_P and w'_{nf} are the weight fraction of the dry polymer and non-freezable water in the polymer phase, respectively.

Figure 7 compares the determined and modeled $T_{g,S}$ values and indicates that the Gordon-Taylor equation adequately describes the effect of the non-freezable water on the $T_{g,S}$. The K has a value ranging from 0.9 to 2.1, which is consistent with the literature (1-3) [68]. Interestingly, two neutral polymers (i.e., XLPEGDA and PEGDA-*co*-PEGMEA) exhibit similar K values (~2.1), and

the K value decreases to 1.3 for PEGDA-*co*-SBMA, 1.1 for PEGDA-*co*-AX, and 0.9 for PEGDA-*co*-CX. The K can be estimated using the following equation [68, 69].

$$K = \frac{\alpha_l - \alpha_g}{\alpha_W} = \frac{\Delta\alpha}{\alpha_W} \tag{14}$$

where α_l and α_g are the thermal expansion coefficient of the polymer at rubbery and glass state, respectively. The α_W is the thermal expansion coefficient for the amorphous ice. Based on the Simha and Boyer rule ($\Delta\alpha \cdot T_g$ = constant) [68, 70], polymers with lower $T_{g,P}$ should have higher $\Delta\alpha$ values and thus K values. As shown in Table 1, the increasing order of the $T_{g,P}$ is consistent with the decreasing order of the K values.

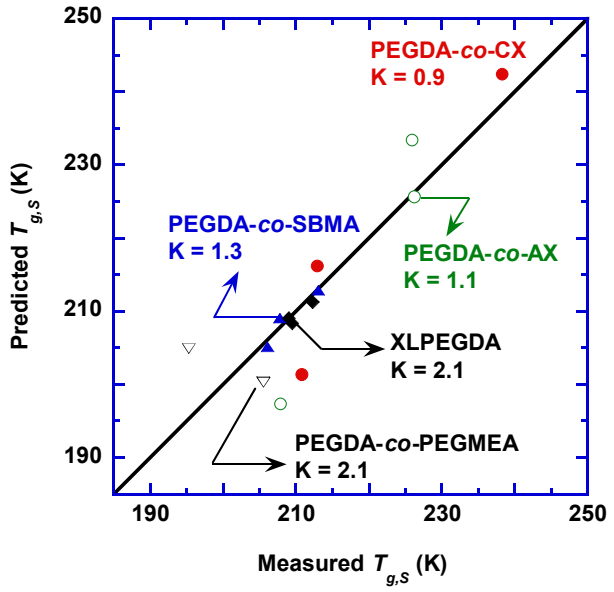

Figure 7. Comparison of the experimental $T_{g,S}$ values with the modeled values using the Gordon-Taylor equation.

3.4. Correlation of water sorption and the NaCl transport properties

Figure 8 compares the correlation between the NaCl diffusion coefficient and the total water fraction or freezable water fraction in the hydrated polymers. The modified Yasuda equation

(Eq. (1)) satisfactorily captures the effect of both total water and freezable water on the NaCl diffusivity [26]. On the other hand, the correlation with the total water is better than that with the freezable water. The b value of 2.4 from the correlation with v_w is similar to the literature value (2.39) [26]. More importantly, the modeling with the freezable water deviates significantly at the low fractional volume of the freezable water because the non-freezable water becomes more significant. This result is also consistent with the observation that Nafion still exhibits significant proton conductivity at temperatures as low as -50 °C, where the freezable water crystallizes [12]. The non-freezable water may be dynamically exchangeable with the freezable water and thus contribute to the ion diffusion, and the correlation of the salt diffusivity with the total water is reasonable.

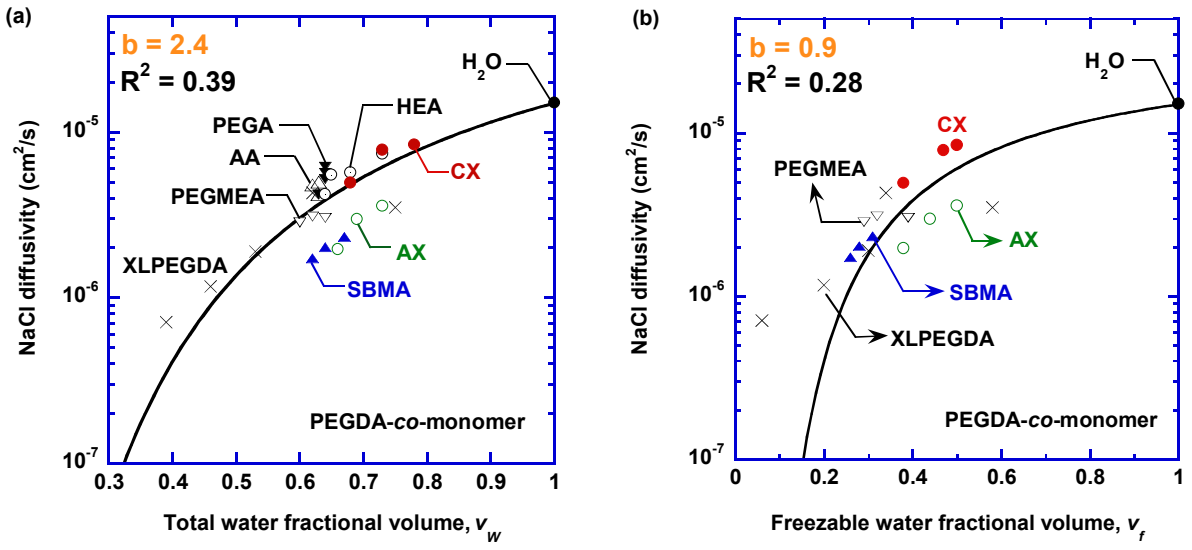

Figure 8. Diffusion coefficient as a function of (a) total water and (b) freezable water fractional volume in the polymer networks. The salt diffusivity of PEG-based copolymers containing acrylic acid (AA), poly(ethylene glycol) acrylate (PEGA, M_n=380), and 2-hydroxyethyl acrylate (HEA) was obtained from the literature [22, 40].

Figure 9 presents the correlation of the NaCl solubility with the volume fraction of the total water or freezable water in the hydrated polymer. In the absence of specific interactions between the polymers and salt, the salt can only be soluble in the water in the hydrogels, instead of the polymer phase. The salt concentration in the polymer (C_S^m) equals to $C_S v_W$ or $C_S v_f$, and the salt solubility equals to v_W or v_f based on Eq. (11), indicating that the water in the hydrated polymers behaves as the bulk water (as demonstrated by the parity line) [5, 47]. Therefore, Fig. 9a shows that the determined salt solubility is significantly below the parity line, even for the neutral polymers, indicating that not all the water in the polymers contributes to the salt dissolution equally. The charged polymers exhibit much lower salt solubility than neutral or zwitterionic polymers at the same v_W values, presumably due to the interaction between co-ions and counter-ions [71].

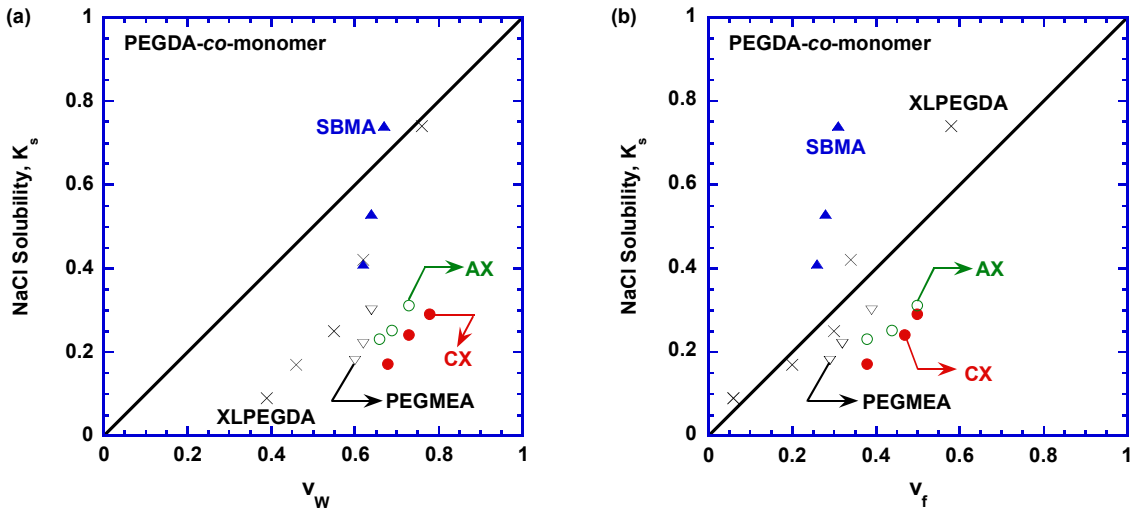

Figure 9. NaCl solubility (K_S) as a function of (a) the volume fraction of total water (v_W) and (b) the volume fraction of the freezable water (v_f) in the hydrated polymers at 21 ºC.

Figure 9b shows that the salt solubility in neutral polymers (XLPEGDA and PEGDA-*co*-PEGMEA) is almost the same as the v_f, suggesting that the non-freezable water does not participate in the salt dissolvation, and intermediate water behaves similarly to the free water. The NaCl solubility in the charged polymers is slightly below the parity line due to the Donnan effect [30, 71]. On the other hand, the NaCl solubility in the zwitterionic PEGDA-*co*-SBMA) increases rapidly with increasing water content presumably, presumably because of the favorable electrostatic interactions between the fixed charge groups and their corresponding counterions [22, 29].

4. CONCLUSION

We systematically investigate the effect of the states of water on the ion sorption and diffusion in four series of hydrated polymers, neutral PEGDA-*co*-PEGMEA copolymers, zwitterionic PEGDA-*co*-SBMA, cation exchange PEGDA-*co*-CX, and anion exchange PEGDA-*co*-AX. Increasing the PEGDA content in the polymers increases the cross-linking density, decreasing the contents of the free water and non-freezable water and salt diffusivity and increasing the intermediate water content. The charged polymers exhibit much higher water sorption and free water content than the neutral and zwitterionic ones. The PEGDA-*co*-SBMA copolymers exhibit water uptake and free water content similar to PEGDA-*co*-PEGMEA, but much higher non-freezable water content. The number of non-freezable water molecules is 1.9 per EO repeating unit, 17 per SBMA, 15 per AMPS, and 9.1 per AETMAC, in agreement with some literature studies.

The T_g of the hydrated polymers is satisfactorily correlated with the non-freezable water using the Gordon-Taylor model, confirming that polymer and non-freezable water should be considered as one phase and separated from the free and intermediate water. The salt solubility in the neutral polymers is similar to the volume fraction of the freezable water, indicating that the non-freezable water does not participate in the dissolution of salt. The NaCl diffusion coefficient can be correlated with the total water using the single-parameter Yasuda model, suggesting that the non-freezable water also play a significant role in the NaCl diffusion. This study signifies that each water state affects the polymer properties differently, which needs to be considered when designing materials with controlled ion transport properties.

SUPPORTING INFORMATION

Correlation between W_{im} and W_W, and between Wim and the percentage of W_{free} in W_W or W_f. Summary of water uptake and the amount of water at different states as well as its contribution to the total water uptake in the four series hydrated copolymers.

ACKNOWLEDGMENTS

We gratefully acknowledge the support from the U.S. National Science Foundation (NSF) Division of Civil, Mechanical, and Manufacturing Innovation (CMMI) with a grant number of 1635026.

REFERENCES

[1] H.B. Park, J. Kamcev, L.M. Robeson, M. Elimelech, B.D. Freeman, Maximizing the right stuff: The trade-off between membrane permeability and selectivity, Science, 356 (2017) eaab0530.

[2] G.M. Geise, H.S. Lee, D.J. Miller, B.D. Freeman, J.E. Mcgrath, D.R. Paul, Water purification by membranes: the role of polymer science, J. Polym. Sci., Part B: Polym. Phys., 48 (2010) 1685-1718.

[3] J.R. Werber, C.O. Osuji, M. Elimelech, Materials for next-generation desalination and water purification membranes, Nat. Rev. Mater., 1 (2016) 16018.

[4] D.L. Shaffer, J.R. Werber, H. Jaramillo, S. Lin, M. Elimelech, Forward osmosis: Where are we now?, Desalination, 356 (2015) 271-284.

[5] S. Zhao, K. Huang, H. Lin, Impregnated membranes for water purification using forward osmosis, Ind. Eng. Chem. Res., 54 (2015) 12354-12366.

[6] A.W. Mohammad, Y.H. Teow, W.L. Ang, Y.T. Chung, D.L. Oatley-Radcliffe, N. Hilal, Nanofiltration membranes review: Recent advances and future prospects, Desalination, 356 (2015) 226-254.

[7] D.J. Miller, D. Dreyer, C. Bielawski, D.R. Paul, B.D. Freeman, Surface modification of water purification membranes: A review, Angew. Chem. Int. Ed., 56 (2016) 4662-4711.

[8] N. Shahkaramipour, T.N. Tran, S. Ramanan, H. Lin, Membranes with surface-enhanced antifouling properties for water purification, Membranes, 7 (2017) 13.

[9] H. Strathmann, Electrodialysis, a mature technology with a multitude of new applications, Desalination, 264 (2010) 268-288.

[10] M. Galizia, W.S. Chi, Z.P. Smith, T.C. Merkel, R.W. Baker, B.D. Freeman, 50th anniversary perspective: polymers and mixed matrix membranes for gas and vapor separation: a review and prospective opportunities, Macromolecules, 50 (2017) 7809-7843.

[11] G. Merle, M. Wessling, K. Nijmeijer, Anion exchange membranes for alkaline fuel cells: A review, J. Membr. Sci., 377 (2011) 1-35.

[12] A. Kusoglu, A.Z. Weber, New insights into perfluorinated sulfonic-acid ionomers, Chem. Rev., 117 (2017) 987-1104.

[13] S. Gottesfeld, D.R. Dekel, M. Page, C. Bae, Y.S. Yan, P. Zelenay, Y.S. Kim, Anion exchange membrane fuel cells: Current status and remaining challenges, J. Power Sources, 375 (2018) 170-184.

[14] H. Lin, T. Kai, B.D. Freeman, S. Kalakkunnath, D.S. Kalika, The effect of cross-linking on gas permeability in cross-linked poly(ethylene glycol diacrylate), Macromolecules, 38 (2005) 8381-8393.

[15] Y.H. Wu, H.B. Park, T. Kai, B.D. Freeman, D.S. Kalika, Water uptake, transport and structure characterization in poly(ethylene glycol) diacrylate hydrogels, J. Membr. Sci., 347 (2010) 197-208.

[16] W. Xie, H. Ju, G.M. Geise, B.D. Freeman, J.I. Mardel, A.J. Hill, J.E. McGrath, Effect of free volume on water and salt transport properties in directly copolymerized disulfonated poly(arylene ether sulfone) random copolymers, Macromolecules, 44 (2011) 4428-4438.

[17] H.B. Park, B.D. Freeman, Z.B. Zhang, M. Sankir, J.E. McGrath, Highly chlorine-tolerant polymers for desalination, Angew. Chem. Int. Ed. Engl., 47 (2008) 6019-6024.

[18] J. Kamcev, R. Sujanani, E.S. Jang, N. Yan, N. Moe, D.R. Paul, B.D. Freeman, Salt concentration dependence of ionic conductivity in ion exchange membranes, J. Membr. Sci., 547 (2018) 123-133.

[19] J. Kamcev, D.R. Paul, G.S. Manning, B.D. Freeman, Predicting salt permeability coefficients in highly swollen, highly charged ion exchange membranes, ACS Appl. Mater. Interfaces, 9 (2017) 4044-4056.

[20] J. Kamcev, D.R. Paul, B.D. Freeman, Ion activity coefficients in ion exchange polymers: applicability of Manning's counterion condensation theory, Macromolecules, 48 (2015) 8011-8024.

[21] Q.F. An, Y.L. Ji, W.S. Hung, K.R. Lee, C.J. Gao, AMOC positron annihilation study of zwitterionic nanofiltration membranes: correlation between fine structure and ultrahigh permeability, Macromolecules, 46 (2013) 2228-2234.

[22] S. Shah, J. Liu, S. Ng, S. Luo, R. Guo, C. Cheng, H. Lin, Transport properties of small molecules in zwitterionic polymers, J. Polym. Sci., Part B: Polym. Phys., 54 (2016) 1924-1934.

[23] G.M. Geise, H.B. Park, A.C. Sagle, B.D. Freeman, J.E. McGrath, Water permeability and water/salt selectivity tradeoff in polymers for desalination, J. Membr. Sci., 369 (2011) 130-138.

[24] M.A. Hickner, Water-mediated transport in ion-containing polymers, J. Polym. Sci., Part B: Polym. Phys., 50 (2012) 9-20.

[25] G.M. Geise, D.R. Paul, B.D. Freeman, Fundamental water and salt transport properties of polymeric materials, Prog. Polym. Sci., 39 (2014) 1-24.

[26] H. Zhang, G.M. Geise, Modeling the water permeability and water/salt selectivity tradeoff in polymer membranes, J. Membr. Sci., 520 (2016) 790-800.

[27] H. Yasuda, C. Lamaze, L. Ikenberry, Permeability of solutes through hydrated polymer membranes. Part I. Diffusion of sodium chloride, Macromol. Chem. Phys., 118 (1968) 19-35.

[28] N. Yan, D.R. Paul, B.D. Freeman, Water and ion sorption in a series of cross-linked AMPS/PEGDA hydrogel membranes, Polymer, 146 (2018) 196-208.

[29] L. Ni, J. Meng, G.M. Geise, Y. Zhang, J. Zhou, Water and salt transport properties of zwitterionic polymers film, J. Membr. Sci., 491 (2015) 73-81.

[30] J. Kamcev, M. Galizia, F.M. Benedetti, E.S. Jang, D.R. Paul, B.D. Freeman, G.S. Manning, Partitioning of mobile ions between ion exchange polymers and aqueous salt solutions: importance of counter-ion condensation, Phys. Chem. Chem. Phys., 18 (2016) 6021-6031.

[31] T. Nakajima, H. Sato, Y. Zhao, S. Kawahara, T. Kurokawa, K. Sugahara, J.P. Gong, A universal molecular stent method to toughen any hydrogels based on double network concept, Adv. Funct. Mater., 22 (2012) 4426-4432.

[32] Z.H. Ping, Q.T. Nguyen, S.M. Chen, J.Q. Zhou, Y.D. Ding, States of water in different hydrophilic polymers - DSC and FTIR studies, Polymer, 42 (2001) 8461-8467.

[33] J. Rault, The state of water in swollen polymers, Macromol. Symp., 100 (1995) 31-38.

[34] K. Nagai, S. Tanaka, Y. Hirata, T. Nakagawa, M.E. Arnold, B.D. Freeman, D. Leroux, D.E. Betts, J.M. DeSimone, F.A. DiGiano, Solubility and diffusivity of sodium chloride in phase-separated block copolymers of poly (2-dimethylaminoethyl methacrylate), poly (1, 1′-dihydroperfluorooctyl methacrylate) and poly (1, 1, 2, 2-tetrahydroperfluorooctyl acrylate), Polymer, 42 (2001) 09941-09948.

[35] M.B. Ahmad, M.B. Huglin, DSC studies on states of water in crosslinked poly(methyl methacrylate-co-N-vinyl-2-pyrrolidone) hydrogels, Polym. Int., 33 (1994) 273-277.

[36] M. Tanaka, A. Mochizuki, Clarification of the blood compatibility mechanism by controlling the water structure at the blood–poly(meth)acrylate interface, J. Biomater. Sci., Polym. Ed., 21 (2010) 1849-1863.

[37] M. Tanaka, A. Mochizuki, N. Ishii, T. Motomura, T. Hatakeyama, Study of blood compatibility with poly(2-methoxyethyl acrylate): Relationship between water structure and platelet compatibility in poly(2-methoxyethylacrylate-co-2-hydroxyethylmethacrylate), Biomacromolecules, 3 (2002) 36-41.

[38] T.N. Tran, S.N. Ramanan, H. Lin, Synthesis of hydrogels with antifouling properties as membranes for water purification, J. Vis. Exp., (2017) DOI: 10.3791/55426.

[39] H. Ju, B.D. McCloskey, A.C. Sagle, Y.H. Wu, V.A. Kusuma, B.D. Freeman, Crosslinked poly(ethylene oxide) fouling resistant coating materials for oil/water separation, J. Membr. Sci., 307 (2008) 260-267.

[40] A.C. Sagle, H. Ju, B.D. Freeman, M.M. Sharma, PEG-based hydrogel membrane coatings, Polymer, 50 (2009) 756-766.

[41] C. Leng, H.-C. Hung, S. Sun, D. Wang, Y. Li, S. Jiang, Z. Chen, Probing the surface hydration of nonfouling zwitterionic and PEG materials in contact with proteins, ACS Appl. Mater. Interfaces, 7 (2015) 16881-16888.

[42] S. Jiang, Z. Cao, Ultralow-fouling, functionalizable, and hydrolyzable zwitterionic materials and their derivatives for biological applications, Adv. Mater., 22 (2010) 920-932.

[43] H. Ju, B.D. McCloskey, A.C. Sagle, V.A. Kusuma, B.D. Freeman, Preparation and characterization of crosslinked poly(ethylene glycol) diacrylate hydrogels as fouling-resistant membrane coating materials, J. Membr. Sci., 330 (2009) 180-188.

[44] T. Hatakeyma, H. Kasuga, M. Tanaka, H. Hatakeyama, Cold crystallization of poly(ethylene glycol)–water systems, Thermochim. Acta, 465 (2007) 59-66.

[45] I.I. Katkov, F. Levine, Prediction of the glass transition temperature of water solutions: comparison of different models, Cryobiology, 49 (2004) 62-82.

[46] S.J. Lue, S.J. Shieh, Modeling water states in polyvinyl alcohol-fumed silica nano-composites, Polymer, 50 (2009) 654-661.

[47] H. Ju, A.C. Sagle, B.D. Freeman, J.I. Mardel, A.J. Hill, Characterization of sodium chloride and water transport in crosslinked poly(ethylene oxide) hydrogels, J. Membr. Sci., 358 (2010) 131-141.

[48] H. Lin, E. Van Wagner, B.D. Freeman, L.G. Toy, R.P. Gupta, Plasticization-enhanced hydrogen purification using polymeric membranes, Science, 311 (2006) 639-642.

[49] N. Paranjape, P.C. Mandadapu, G. Wu, H. Lin, Highly-branched cross-linked poly(ethylene oxide) with enhanced ionic conductivity, Polymer, 111 (2017) 1-8.

[50] T. Wu, F.L. Beyer, R.H. Brown, R.B. Moore, T.E. Long, Influence of zwitterions on thermomechanical properties and morphology of acrylic copolymers: Implications for electroactive applications, Macromolecules, 44 (2011) 8056-8063.

[51] A. Higuchi, T. Iijima, D.S.C. investigation of the states of water in poly(vinyl alcohol) membranes, Polymer, 26 (1985) 1207-1211.

[52] T. Hatakeyama, M. Tanaka, H. Hatakeyama, Studies on bound water restrained by poly(2-methacryloyloxyethyl phosphorylcholine): Comparison with polysaccharide–water systems, Acta Biomater., 6 (2010) 2077-2082.

[53] Z. Zhang, T. Chao, S. Chen, S. Jiang, Superlow fouling sulfobetaine and carboxybetaine polymers on glass slides, Langmuir, 22 (2006) 10072-10077.

[54] G. Cheng, G. Li, H. Xue, S. Chen, J.D. Bryers, S. Jiang, Zwitterionic carboxybetaine polymer surfaces and their resistance to long-term biofilm formation, Biomaterials, 30 (2009) 5234-5240.

[55] T. de Vringer, J.G.H. Joosten, H.E. Junginger, A study of the hydration of polyoxyethylene at low temperatures by differential scanning calorimetry, Colloid. Polym. Sci., 264 (1986) 623-630.

[56] S.L. Hager, T.B. Macrury, Investigation of phase behavior and water binding in poly(alkylene oxide) solutions, J. Appl. Polym. Sci., 25 (2003) 1559-1571.

[57] J. Wu, W. Lin, Z. Wang, S. Chen, Y. Chang, Investigation of the hydration of nonfouling material poly(sulfobetaine methacrylate) by low-field Nuclear Magnetic Resonance, Langmuir, 28 (2012) 7436-7441.

[58] S. Lüsse, K. Arnold, The interaction of poly(ethylene glycol) with water studied by ^{1}H and ^{2}H NMR relaxation time measurements, Macromolecules, 29 (1996) 4251-4257.

[59] Q. Shao, Y. He, A.D. White, S. Jiang, Difference in hydration between carboxybetaine and sulfobetaine, J. Phys. Chem. B, 114 (2010) 16625-16631.

[60] A. Siu, J. Schmeisser, S. Holdcroft, Effect of Water on the Low Temperature Conductivity of Polymer Electrolytes, J. Phys. Chem. B, 110 (2006) 6072-6080.

[61] H. Ma, Hydration structure of Na^+, K^+, F^-, and Cl^- in ambient and supercritical water: A quantum mechanics/molecular mechanics study, Int. J. Quantum Chem., 114 (2014) 1006-1011.

[62] H. Sakuma, T. Kondo, H. Nakao, K. Shiraki, K. Kawamura, Structure of hydrated sodium ions and water molecules adsorbed on the mica/water interface, J. Phys. Chem. C, 115 (2011) 15959-15964.

[63] Q. Shao, S. Jiang, Molecular understanding and design of zwitterionic materials, Adv. Mater., 27 (2015) 15-26.

[64] D.H. Powell, A.C. Barnes, J.E. Enderby, G.W. Neilson, P.S. Salmon, The hydration structure around chloride ions in aqueous solution, Faraday Discuss. Chem. Soc., 85 (1988) 137-146.

[65] B.C. Hancock, B.C. Hancock, G. Zografi, G. Zografi, The relationship between the glass transition temperature and the water content of amorphous pharmaceutical solids, Pharm. Res., 11 (1994) 471-477.

[66] D. Lourdin, L. Coignard, H. Bizot, P. Colonna, Influence of equilibrium relative humidity and plasticizer concentration on the water content and glass transition of starch materials, Polymer, 38 (1997) 5401-5406.

[67] B. Lam, M. Wei, L. Zhu, S. Luo, R. Guo, A. Morisato, P. Alexandridis, H. Lin, Cellulose triacetate doped with ionic liquids for membrane gas separation, Polymer, 89 (2016) 1-11.

[68] D.W. Van Krevelen, K. Te Nijenhuis, Properties of Polymers: Their Correlation with Chemical Structure: Their Numerical Estimation and Prediction from Additive Group Contributions, Elsevier, Amsterdam, 2009.

[69] J.V. Dawkins, Developments in Polymer Characterisation—4, Springer Netherlands, 2012.

[70] R. Simha, R.F. Boyer, On a General Relation Involving the Glass Temperature and Coefficients of Expansion of Polymers, J. Chem. Phys., 37 (1962) 1003-1007.

[71] J. Kamcev, D.R. Paul, B.D. Freeman, Effect of fixed charge group concentration on equilibrium ion sorption in ion exchange membranes, J. Mater. Chem. A, 5 (2017) 4638-4650.